The Effects of Propellant Slosh Dynamics on the Solar Dynamics Observatory

Paul Mason[1], Scott R. Starin[1]
NASA Goddard Space Flight Center, Greenbelt, MD, 20771

The Solar Dynamics Observatory (SDO) mission, which is part of the Living With a Star program, was successfully launched and deployed from its Atlas V launch vehicle on February 11, 2010. SDO is an Explorer-class mission now operating in a geosynchronous orbit (GEO). The basic mission is to observe the Sun for a very high percentage of the 5-year mission (10-year goal) with long stretches of uninterrupted observations and with constant, high-data-rate transmission to a dedicated ground station located in White Sands, New Mexico. Almost half of SDO's launch mass was propellant, contained in two large tanks. To ensure performance with this amount of propellant, a slosh analysis was performed prior to launch. This paper provides an overview of the SDO slosh analysis, the on-orbit experience, and the lessons learned.

I. Introduction

SDO is a three-axis controlled, single-fault tolerant spacecraft. The attitude sensor complement[1] includes sixteen coarse sun sensors, a digital sun sensor, three two-axis inertial reference units, two star trackers, and four guide telescopes (Figure 1). Attitude actuation is performed using either four reaction wheels or one of two redundant sets of four attitude thrusters, depending on the control mode. A single main engine provides velocity-change (ΔV) and is controlled by the attitude thrusters. All the attitude thrusters are canted 10 deg about the Z axis, with most of their force directed along the X axis to provide redundancy for the main engine for ΔV delivery. The attitude control software, which runs on the main processor, has five nominal control modes: three wheel-based modes and two thruster-based modes. A wheel-based Safehold, which improve the robustness of the system as a whole, runs on the Attitude Control Electronics (ACE) box to. All six modes are designed on the same basic proportional-integral-derivative attitude control structure, with coarse pointing modes setting their integral gains to zero.

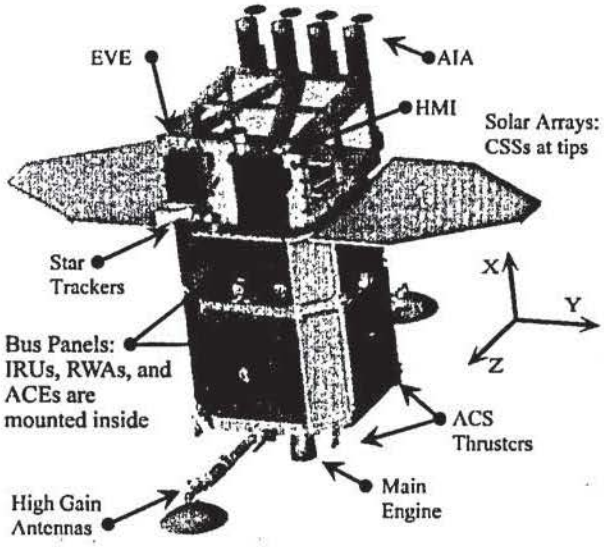

Figure 1. SDO Attitude Control System Hardware[1]

[1] AIAA Senior Member

To achieve and maintain a geosynchronous orbit for a 2974 kg spacecraft in a cost effective manner, the SDO team designed a high-efficiency propulsive system. This bi-propellant design includes a 110 lbf main engine and eight 5 lbf attitude control thrusters[1]. The main engine provides high specific impulse for the maneuvers to attain geosynchronous orbit (GEO), while the smaller Attitude Control System (ACS) thrusters manage the disturbance torques of the larger main engine and can also precisely deliver much smaller orbit adjustments. When the ACS thrusters are used for ΔV without firing the main engine, the four thrusters in one set are commanded to fire continuously except for brief pauses to effectuate attitude control; this is referred to as off-pulsing for control, whereas the ACS thrusters are on-pulsed for control when the main engine is firing. SDO's large solar profile produces large solar torque disturbances and momentum buildup. This buildup drives the frequency of momentum unloads via ACS thrusters. SDO requires 1409 kg of propellant to achieve and maintain the GEO orbit while performing the momentum unloads for 10 years.

For missions requiring large amounts of propellant for orbit insertion and maintenance or momentum unloading, it is imperative that slosh dynamics, the motion of any free liquid propellant surface inside the propellant tanks and its impact on the spacecraft, are understood. Propellant motion can result in periodic disturbance forces and torques acting on a spacecraft or launch vehicle. These slosh effects must be accounted for in the control mode design. A poor controller design can excite the slosh dynamics, which can adversely impact the performance and stability of the spacecraft. Due to the higher levels of linear and angular accelerations, slosh effects on the spacecraft are more prevalent during the thruster-based modes (DeltaH and DeltaV).

The initial plan to carry SDO from its initial geosynchronous-transfer orbit (GTO) with a perigee of 8,800 km to its final geosynchronous circular orbit consisted of ten maneuvers conducted over a period of three weeks: one engineering burn, then six apogee motor firings (AMFs) for which the primary ΔV would come from the main engine, followed by three trim motor firing (TMFs) performed using ACS thrusters only. The engineering burn was designed as a short dress rehearsal for a full apogee motor firing. In the engineering burn and in each of the AMFs, the first 20 seconds of the burn would use ACS thrusters only, with thrusters off-pulsing for attitude control, and was meant as a settling burn to allow the propellant to settle to the bottom of the tanks before the main engine fired. After this settling burn, the main engine fired for the rest of the burn, with the ACS thrusters on-pulsing for attitude control. See Ottenstein[11] for a more complete description of the SDO orbit raising plan.

The following sections provide a brief literature review, a preflight slosh analysis summary, documents the flight experience, catalogs the slosh lessons learned, and provides insight into current and future work.

II. Literature Review

Slosh dynamics has been studied for several decades. Even though most of the work has been in the aerospace industry, slosh dynamics is applicable to industrial/manufacturing applications (movement of fluid-filled containers), civil engineering (earthquakes), automotive engineering (fuel trucks), and ship dynamics. In the case of manufacturing, much of the work in this field is based on slosh due to lateral motion in a 1-g environment. Many companies now utilize computational fluid dynamics (CFD) analysis to account for and mitigate the effects of slosh.

The largest body of slosh dynamics and suppression work is found in the aerospace industry. Some of the earliest works in slosh were associated with vehicle stability for launch vehicles, missiles and spacecraft[2]. As vehicle size and propellant capacity increase, the potential for slosh increases significantly. The coupling between the slosh and vehicle dynamics can lead to instability or poor performance. With the advent of larger aerospace vehicles and tighter pointing requirements, analyzing and controlling the slosh dynamics has become a standard component in the analysis and design of many aerospace vehicles.

Based on the modeling techniques, most of the work in slosh modeling can be categorized into two areas: fluid dynamics modeling and equivalent mechanical models. The fluid dynamics modeling can be broken into two sub-categories: analytic solutions and computational methods (e.g. smooth partial hydrodynamics (SPH), which is analogous to finite elements in structures). Analytic modeling of slosh dynamics uses partial differential equations to describe fluid behavior in a given environment. H. Norman Abramson, a distinguished researcher in the area of slosh dynamics, published a document[3] that describes the analytic process for determining the slosh dynamics for a given container shape. As he states, "an exact solution to the general problem of fluid oscillations in a moving container is extremely difficult." For this reason, the initial step is to define any simplifying assumptions. Next, the fundamental fluid dynamics laws are used to define the basic partial differential equations (PDE). The boundary conditions, which are determined as a function of the container shape, are incorporated into the PDEs from the fundamental laws. In many cases, numerical PDE techniques must be utilized to obtain a solution. In fact, most analytic studies feed into the CFD slosh analysis.

In many applications, analytic solutions are prohibitively complex. Analytic methods are often unpractical for large problems, irregular shapes, and variable fluid compositions and properties. In these situations, numerical techniques such as CFD are usually employed. Since numerical methods are not exact, they may be less accurate than direct analysis of the PDEs. However, direct analysis may require more time to obtain solutions than CFD methods, and a direct solution may even be impossible. Due to the nature of numerical methods, most of the literature is associated with a particular application. As the complexity of the problem increases so does the computational expense. In some cases, the complexity reaches a point where a supercomputer must be used to solve the problem[4].

Equivalent mechanical slosh modeling, described in the next section, provides a simple and empirical, though lower-accuracy, alternative to fluid dynamics methods. Equivalent mechanical models (also called mechanical analogy models) are particularly useful when designing a control system or creating a model based on solid-body dynamics for stability or performance analyses. In the aerospace industry, equivalent slosh models have been used since the 1960's. In many cases, these equivalent models are an assemblage of dampers or dashpots, springs, and masses. More complicated models incorporate camshafts, slides, and nonlinear elements[5] to simulate a desired motion. In 1964, Roberts, Basurto and Chen[6] compiled a slosh design handbook with many equivalent mechanical models, including some of their own design, and their parameters. The accuracy of an equivalent model is a function of the validity of the model for the given container shape, fluid properties (e.g. laminar flow, accelerations), and the model parameters. The equivalent mechanical model parameters can be derived from analytic expressions or from parameter estimation of flight or numerical data. In general, choice of modeling technique is a tradeoff between simplicity and accuracy.

III. Preflight Analysis

The preflight slosh analysis was based on closed-loop Simulink simulations that utilize an equivalent mechanical model. Due to its simplicity, heritage and visual representation, the equivalent mechanical pendulum slosh model was chosen as the primary modeling technique in this analysis. One of the advantages of the pendulum model is that the slosh motion is constrained to the surface of a sphere. In missile applications, the high acceleration environment forces most of the fuel to the bottom, which is represented by fix fuel mass at the bottom of the tank. The rest of the fuel is modeled as a pendulum. The resulting oscillations are usually small and well defined. For this reason, the pendulum model has primarily been used for fuel slosh with rockets. With the addition of the damping, which is a function of tank geometry and fill fraction, the pendulum model can be used for low-acceleration spacecraft applications. Figure 2 provides a visual description of the pendulum slosh model.

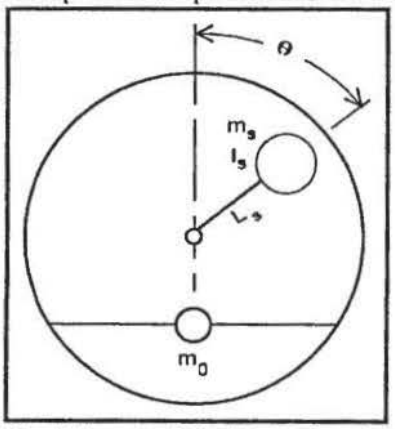

Figure 2. Pendulum model with torsional damping[10]

The equation of motion for the pendulum model with torsional damping is

$$\left(m_s L_s^2 + I_s\right)\ddot{\theta} + C\dot{\theta} - aL_s \sin(\theta) = 0 \tag{1}$$

Where L_s, m_s, I_s, and θ are defined in the figure. a is the axial acceleration The transverse force exerted on the tank (Spacecraft) is

$$F_{axial} = m_s\left(a - L_s\theta^2 \cos\theta + L_s\ddot{\theta}\sin\theta\right) + m_0 a \tag{2}$$

The axial force exerted on the tank (Spacecraft) is

$$F_{transverse} = -m_s\left(L_s\ddot{\theta}\cos\theta + L_s\dot{\theta}^2\sin\theta\right) \tag{3}$$

1. Complex Mechanical Modeling

In general, the equivalent mechanical pendulum model only provides information about the first order dynamics. To capture some of the nonlinear dynamics more complex models are required. Such a model can also account for the coupling of the fuel dynamics to the spacecraft dynamics. London[7] presented a general momentum-based multi-body dynamics model that allows for the coupling between the slosh dynamics and the spacecraft dynamics. This fully coupled model consists of 3 DOF of translation and 3 DOF of rotation. Even though the slosh model component of this formulation does not capture some of the complex nonlinearity, the technique allows for the use of more complex models. Walchko[8] also utilized the momentum based technique to couple the slosh and solar array dynamics with the spacecraft dynamics. In this work, the slosh and the solar array dynamics are modeled with modal parameters such that the higher modes of the slosh can be included in the model. Other works such as Morgenstern[9] have accounted for the coupling between the spacecraft and the slosh dynamics.

A. Preflight Analysis Results

This section provides a summary of the SDO preflight slosh analysis. Most of this analysis was based on the current knowledge and fidelity of the system at the time of the analysis. The purpose of the preflight slosh analysis, which had two levels of fidelity, was to quantify and understand the slosh dynamics. The initial slosh analysis examined the dynamics of slosh in a bare tank configuration, i.e. no propellant management device (PMD). An important product of the bare tank analysis was an initial equivalent mechanical slosh model parameterization, which is a function of the fill fraction and linear acceleration. The bare tank model parameters were used in simulations to determine the impact of slosh on the attitude dynamics during various maneuvers.

The two purposes of the SDO PMD were to prevent gas bubbles from entering the fuel lines and to restrict the motion of the propellant center of mass (CM). Without the PMD the propellant can be located anywhere within the tank and therefore result in a significant shift in the CM location. A large shift in the propellant CM can shift the system CM beyond the required CM envelope, which will result in higher main engine disturbance torques. The CM envelope defines the largest excursion of the CM in any direction that can be tolerated by the ACS for the given main engine force and direction. Gas ingestion, slosh torques and CM shift were the major reasons for adding a PMD to the SDO tanks. At the time of the analysis, the 40% fill fraction was expected to produce the worst case CM shift (Figure 3) and main engine disturbance torques. Only the static CM, which is a function of fill fraction and initial condition, was used in the simulation model. In hindsight, all of the fill fractions should have been examined and the CM dynamics incorporated into the simulation.

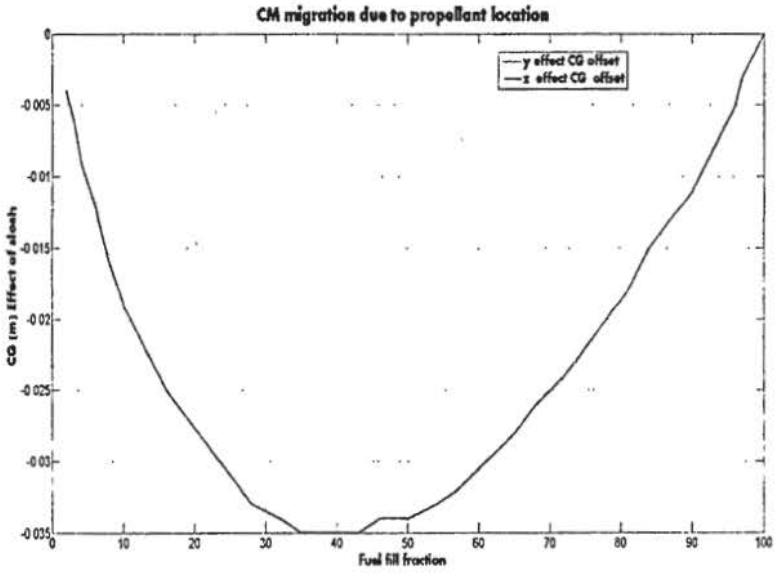

Figure 3. CM variation due to propellant location

With the exception of the damping ratio, the pendulum model parameters were determined using Figure 6.7 in Dodge[10]. The damping ratio was determined based on correspondence with the PMD designer and engineering experience. In order to obtain a better intuitive range, the parameters were compared to parameters in other works. The preflight results were broken up into two cases: slosh dynamics with and without a PMD. The non-PMD case has a damping ratio of 0.2% whereas the PMD case has a damping ratio of 8.0%. Both cases used scaled-mass properties associated with a 40% fill fraction. The mass properties used for this analysis were associated with the configuration in which the high gain antenna was not deployed. The next two subsections provide a summary of the results of the mid-fidelity simulations pendulum model.

1. Case 1: Bare tank

To isolate the effects of slosh on the spacecraft, the only disturbance forces assumed to be acting on the tanks were due to the main engine or ACS thrusters, which were based on the worst case duty cycle analysis and the relatively smaller control torque variations. The external disturbances on the spacecraft were neglected. The initial slosh angle was 90 deg, and model parameters were based on 40% fill fraction and the acceleration levels. Figures 4 and 5 contain a phase-plane plot and slosh torque plot respectively.

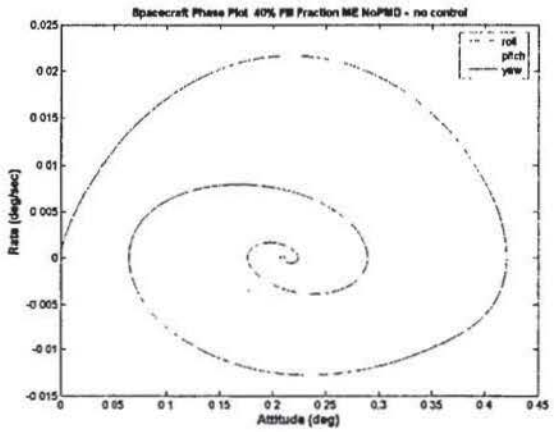

Figure 4. Propellant slosh torques during a main engine maneuver without PMD

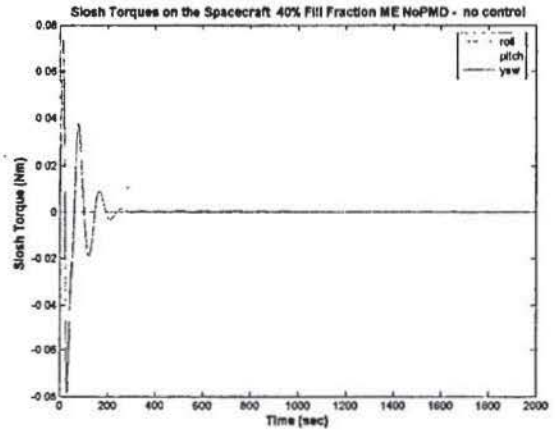

Figure 5. Phase-plane plot during a main engine maneuver without PMD

The peak slosh torque is approximately 0.08 newton-meters (Nm), and the peak attitude and rotational rate errors are 0.44 deg and 0.022 deg/sec respectively. Even though the slosh disturbance torque has a large initial transient, the duration is small. It should also be noted that the slosh torques settle at approximately 500 sec, which is before the main engine is cut off at 1000 sec. In flight or more complex simulations, the damping may not be the same and the slosh torques may settle at a different rate. Next, the PMD case is examined.

2. Case 2 PMD tank

The SDO PMD is designed to ensure zero gas ingestion, increase the damping, and reduce the CM migration due to propellant movement. The results of the main engine burn with a PMD maneuver are provided in the figures below.

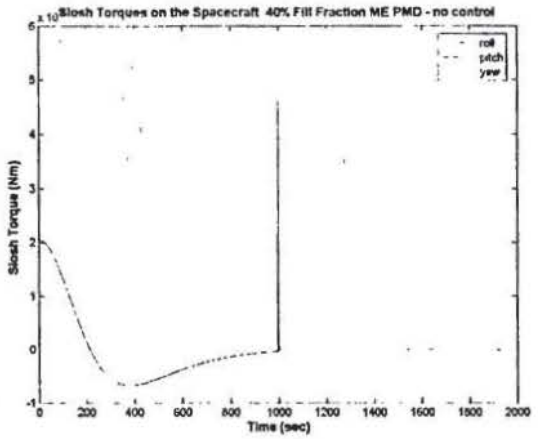

Figure 6. Propellant slosh torques during a main engine burn with a PMD

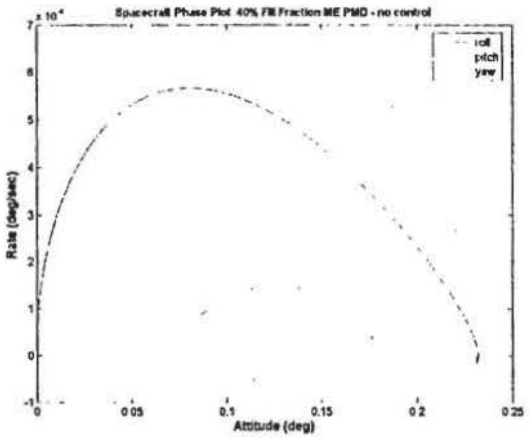

Figure 7. Phase-plane plot for a main engine burn with a PMD

From the figures above, the slosh torques are more damped than the non-PMD case. The slosh starts at 0.0002 Nm and decreases after one overshoot. A sharp transient occurs in the slosh torques when the main engine is turned off at 1000 sec. The attitude and rate errors peak at approximately 0.225 deg and 0.00055 deg/sec respectively. The PMD greatly reduces the disturbance associated with the slosh by at least an order of magnitude.

B. Preflight Conclusions

At the time of the preflight analysis, the simulation results were used to refine and verify requirements, identify control problems, and investigate possible solutions to be included in either the onboard software or ground operation software. For SDO, the resulting slosh dynamics were also the driving factor for the inclusion of the PMD in the tank design redesign of the PMD. The proposed PMD would greatly increase the damping and reduce the center of mass motion, which should improve the stability and performance.

A CFD slosh simulation with the PMD tank was performed by PMD Technology. Even though the simulation was very precise, it required significant computational effort and specialized knowledge, limiting the ability of the SDO project to access fluid dynamics simulations at will for any fill fraction, initial state or input (torques and forces). Furthermore, it was very difficult to incorporate most of these models into closed-loop simulations of the overall spacecraft and its environment. To observe the effects of the slosh dynamics with a PMD, the equivalent mechanical model was updated and used to determine the impact of slosh on the controller performance and stability. In addition, various limits, thresholds, error bars, and the settling burn time, which is part of the maneuver design, were updated based on the second slosh analysis results.

IV. Flight Experience

After a successful launch and Sun Acquisition on February 11, 2010, SDO performed a system checkout, which included an engineering burn. During the engineering burn, which consisted of a 20 second ACS thruster only settling burn and a 60 second main engine burn, there were no observed slosh dynamics due a high fill fraction level (94.65%). The initial Geosynchronous Transfer Orbit (GTO) maneuver plan consisted of five AMF maneuvers using the main engine followed by three TMF maneuvers that only used the ACS thrusters. The next subsections will focus on the pre-anomaly maneuver, the anomaly, the test maneuver and an updated control mode maneuver. As a note, roll, pitch and yaw correspond to axes x, y, and z axis, respectively.

1. AMF 1 burn

After the engineering burn, the first major maneuver was to be the first Apogee Motor Firing (AMF), which consisted of a 20 second settling burn followed by a 19 minute main engine burn. The ACS thrusters are off-pulsed for control during the settling burn and on-pulsed while the main engine is on. At the beginning of AMF 1, the total mass was 2963 kg. The spacecraft slews and settles to the burn attitude. The initial momentum state was approximately 5 Nms and the fill fraction was 95%.

At first glance, attitude and rate errors in Figure 8 were within the requirements. The transition from the settling burn to the main engine burn resulted in an attitude hang-off and a change in frequency, which was expected due to the acceleration difference. In addition, there seemed to be a slight change in frequency and larger change in

magnitude of the attitude errors after 2300 s. The calculated system momentum is the sum of the wheel momentum, the wheel moments of inertia times the reaction wheel tachometer speed, plus the body momentum, the current body moments of inertia times the rates. Figure 9 contains the system momentum magnitude, which drops slightly at the beginning of the maneuver due to the reaction wheels dragging down while the thruster fires to take out momentum imparted by the wheels. The peak system momentum occurs during the settling burn. Based on the roll axis, the system momentum settles within 200 seconds. The dynamic transition was also observed in the system momentum. The slosh disturbance torque (Figure 10) captures the initial slosh spike at approximately 6 Nms and also has the observed transitions. The slosh torque was obtained by subtracting the thruster torque from the derived system torques, which is the derivative of the system momentum. This spike was due to the initial acceleration from the ACS thrusters. Figure 11, a zoomed in version of Figure 10, shows the slosh dynamics settling after 150 sec. Upon closer inspection, a multiple modes can be observed after 1900 seconds. The power spectral density (PSD) was analyzed to determine the frequency of the disturbance torque (Figure 12). The results show that the main disturbance, which was assumed to be slosh, was approximately 0.150 Hz (0.96 rad/sec), which was relatively close to the bare tank natural frequency at that fill fraction. No other frequency can be identified, which contradicts the beat frequency. Throughout the AMF 1 maneuver, the z-axis contains the dominant dynamics followed by the y and x axis.

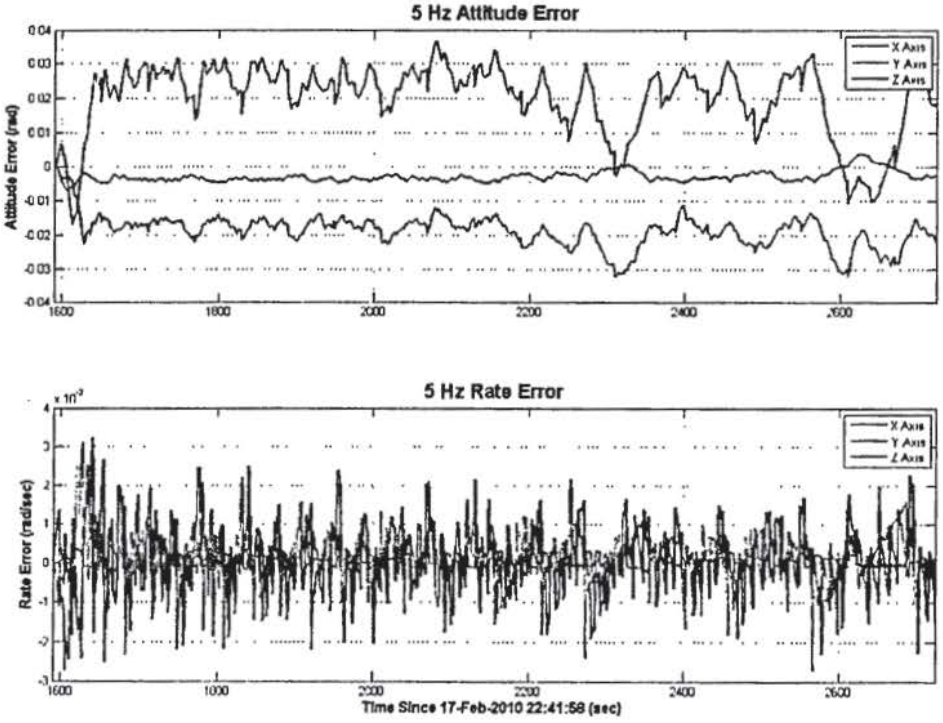

Figure 8. Attitude and Rate errors

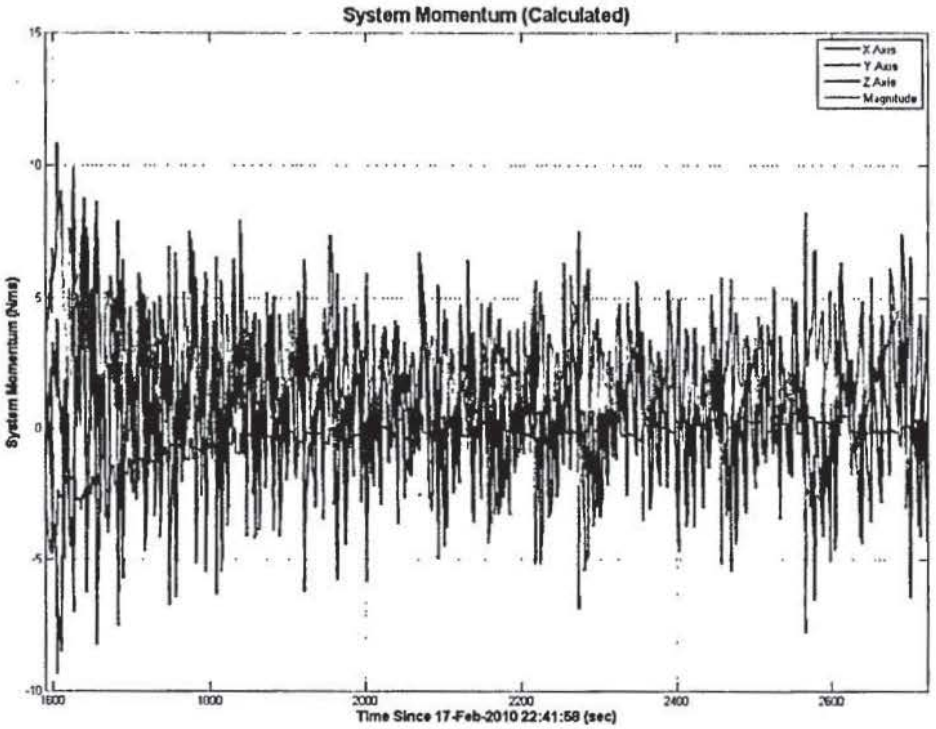

Figure 9. System momentum

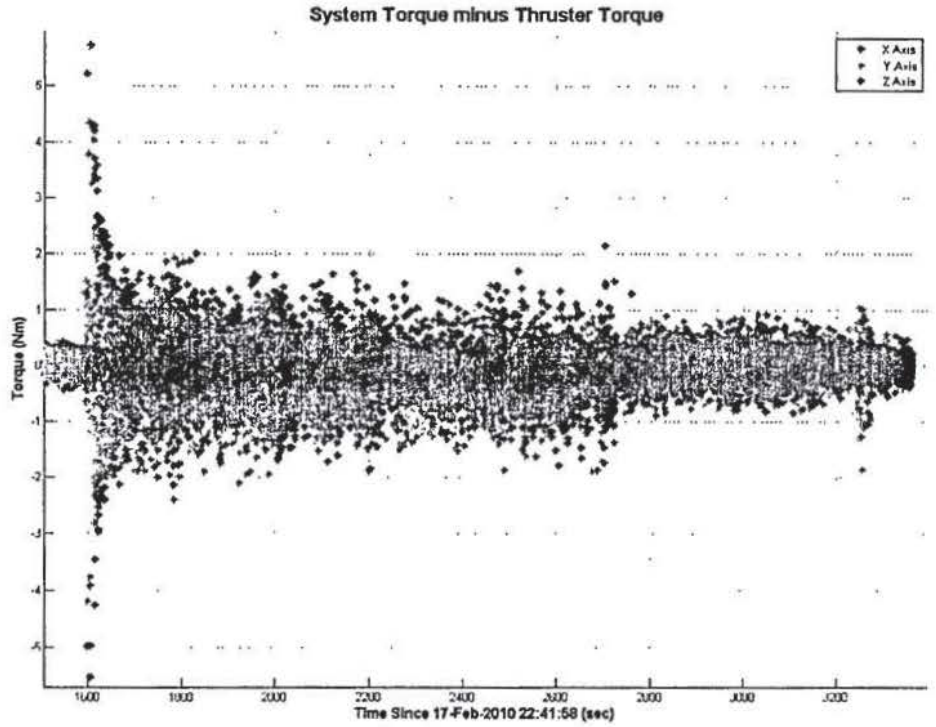

Figure 10. Disturbance torques

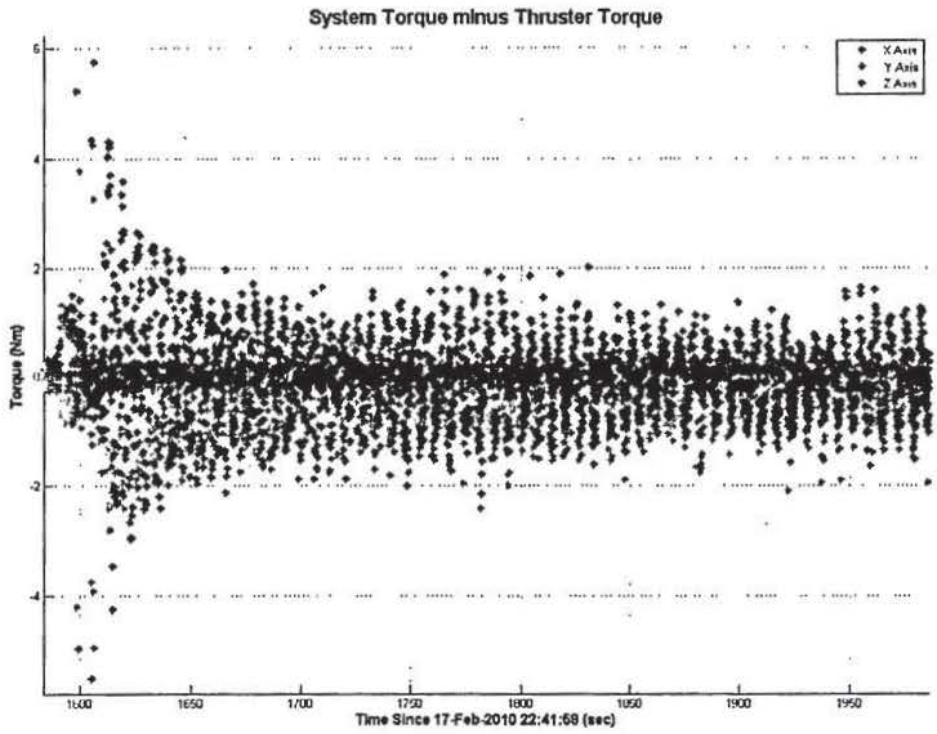

Figure 11. Disturbance torques (zoom)

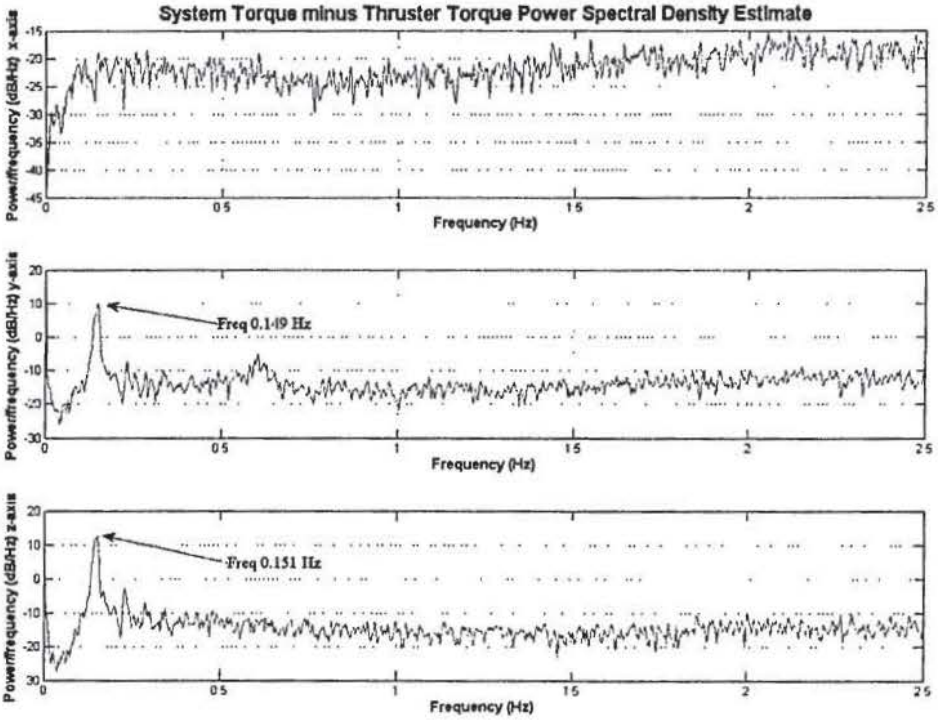

Figure 12. PSD of disturbance torques

2. AMF 2 burn

After the successful completion of AMF 1, it was assumed that the preflight slosh analysis was sufficient and the AMF 2 would be successful. Similar to AMF 1, AMF 2 consisted of a settling burn followed by an 18 minute main engine burn. At the beginning of AMF 2, the total mass was 2786kg. The initial momentum state was approximately 5 Nms and the fill fraction was 81%. The maneuver momentum level was set at 20 Nms. The initial momentum levels were approximately 5 Nms. Thirty-seven seconds after the start of AMF 2, high system momentum levels tripped the FDC limit, which aborted the burn and transition to Sun Acquisition. The resulting attitude/rate error, system momentum, disturbance torque, and disturbance frequency plots are provided in Figures 12-14.

The attitude/rate error, system momentum and disturbance torques all start as in a similar manner to AMF 1. After the completion of the settling burn, a distinct change in the dynamics was observed in the attitude and rate errors (Figure 13), system momentum (Figure 14) and disturbance torques (Figure 15). The z-axis produces the dominant oscillation with an observed damping of approximately 3%. The x-y axis disturbance torque (Figure 15) were larger but within family (<20Nms) of AMF 1. The dominant disturbance frequency of 0.136Hz (0.8589 rad/sec) was identified via PSD analysis (Figure16). This frequency was relatively close to the bare tank natural frequency of 0.847 rad/sec.

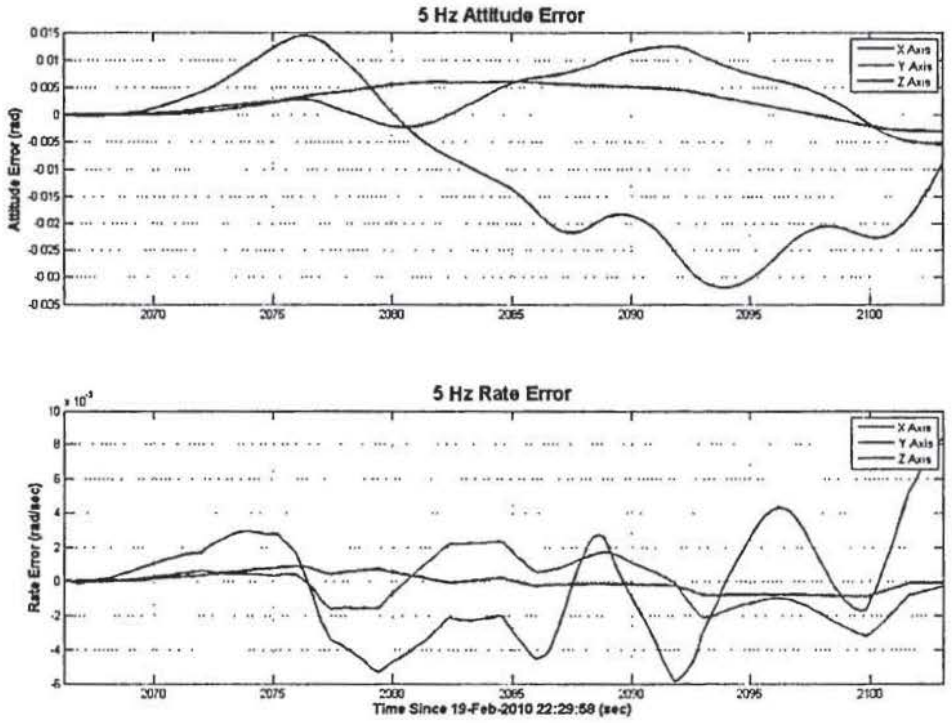

Figure 13. Attitude and Rate errors

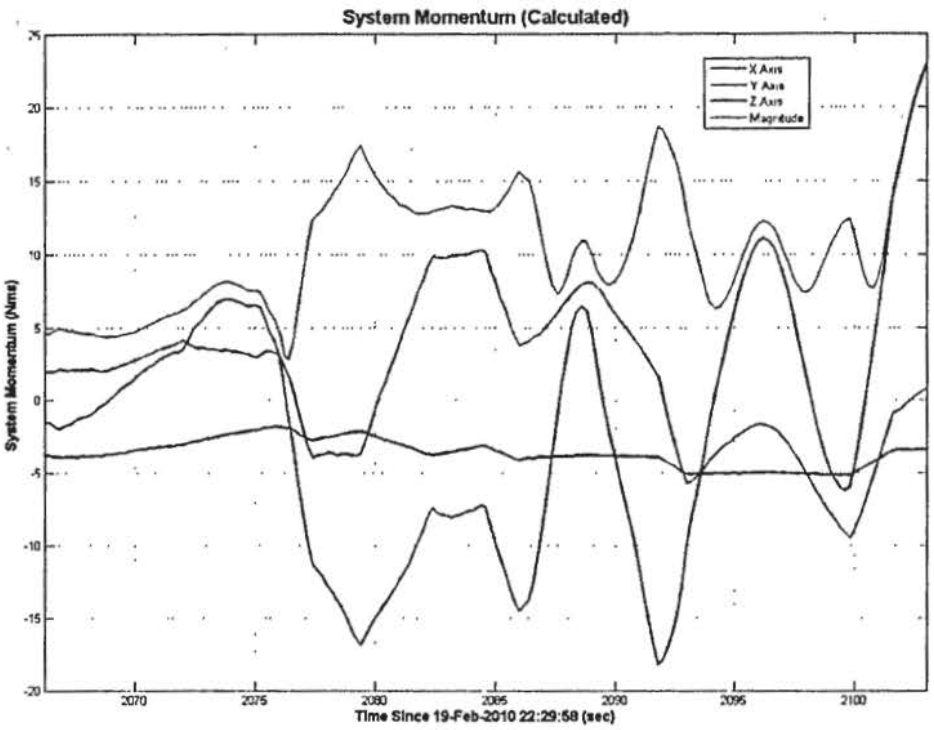

Figure 14. System Momentum

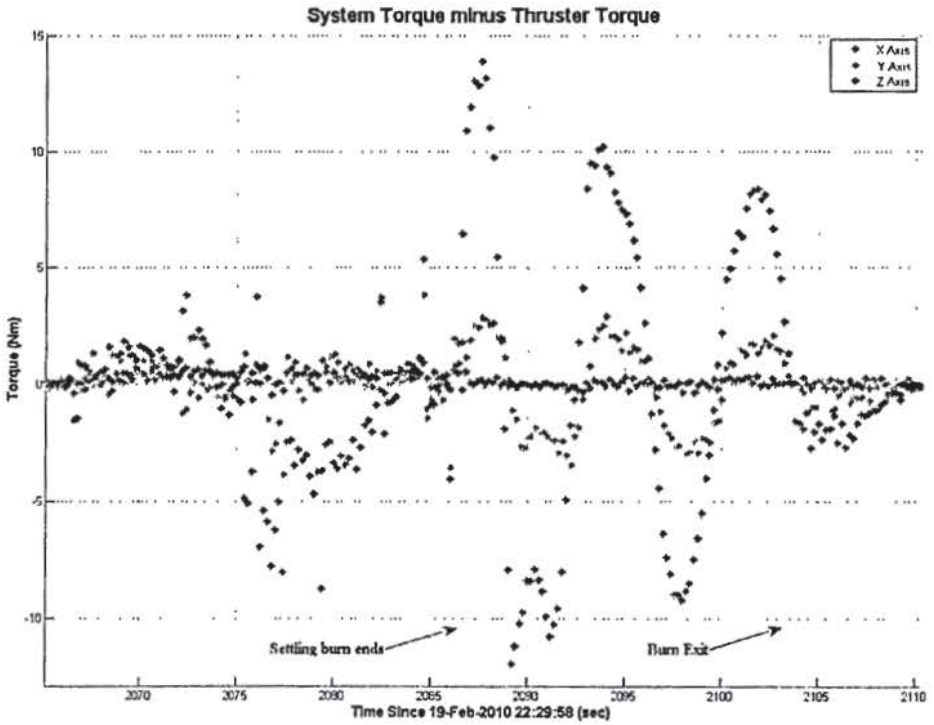

Figure 15. Disturbance torques

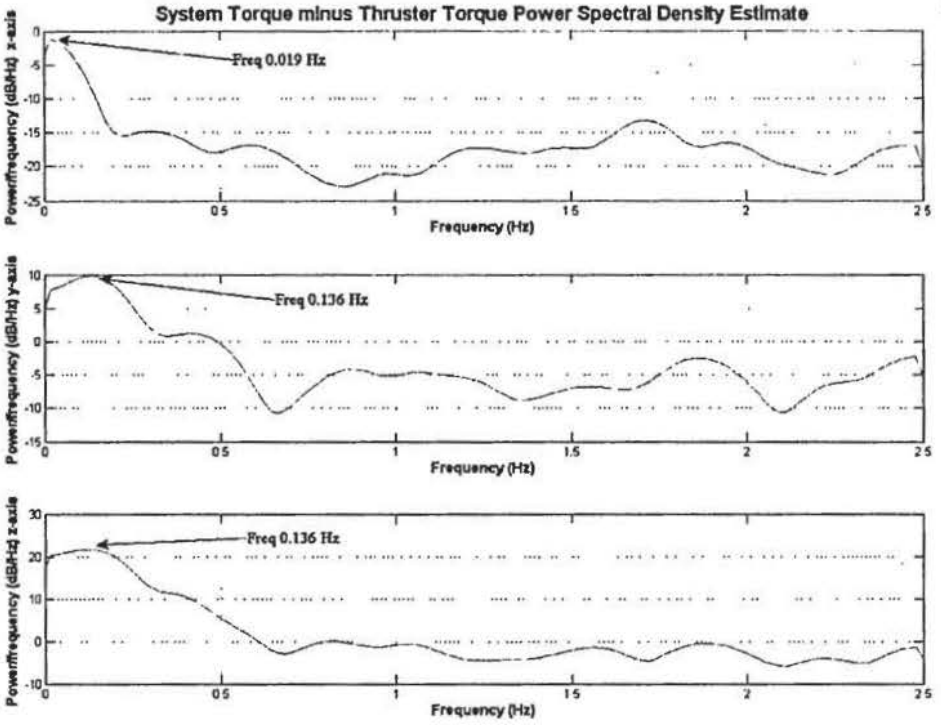

Figure 16. Disturbance torques (zoom)

3. Anomaly Investigation

After the FDC aborted the burn, an anomaly investigation team was formed to determine the root cause and the appropriate mitigation strategy. The anomaly investigation team examined the possible causes including actuator failure (thruster misalignment, thruster failure), sensor failure (sensors provide incorrect information), unexpected disturbance (slosh), controller (controller did not provide the appropriate stabilizing authority), and other failures. This paper only deals with the unexpected disturbance (slosh) investigation. During this investigation, the maneuver team replanned the transfer orbit maneuvers using only ACS thrusters (a back-up mode). Not having the Main Engine delayed getting SDO on orbit by approximately two weeks and required five additional maneuvers.

The initial step of the slosh investigation was to determine if slosh was the root cause. This was accomplished by processing the flight data to remove all known momentum/torque contributors. The remaining dynamics were then characterized and compared with expected slosh dynamics. Plots such as Figures 13 and 14 were used along with thruster firings to determine the applied torques and resulting dynamics. After compiling the data, the results were presented to various experts in propulsion, fluids, controls, systems, and dynamics, who agreed that the observed dynamics were slosh. This conclusion was reached by comparing the observed dynamics with the expected empty tank dynamics and removing all other possible causes.

After the slosh was determined to be the disturbance that caused the anomaly, the prelaunch propellant slosh analysis (inputs, assumptions and method) was reexamined. In addition, the flight data was used to update the preflight slosh model to provide a better correlation to the on orbit observations (damping and frequency). Using this information, the anomaly team suggested three mitigation strategies to account for slosh: lengthen the settling burn, remove the structural filter on the controller, and modify the FDC limit. The initial settling burn time was based on the time needed for the geyser mode, which produces a large nonlinear disturbance torque, to settle. However, it was determined that the geyser mode settling time is not long enough for low frequency propellant motion/disturbances to damp out before the main engine firing. The second suggestion was to disable the Delta-V structural filter, which allowed the mode to meet the design requirement of 12 dB modal suppression of all flexible modes. The structural filter increased the system's phase delay, which affected the Delta-V controller's ability to react to the slosh dynamics. Nulling the structural filter improved the controller's ability to account for slosh. In addition, the on-orbit data suggested the damping was higher than initially predicted. The third suggestion was to increase the FDC limit on system momentum from 20 Nms to 34 Nms. The 20 Nms limit was chosen based on a two-failure scenario (how

much momentum could be placed into the spacecraft by a stuck-on thruster and have the spacecraft successfully recover with one failed wheel); 34 Nms reflected a more realistic failure case.

After the simulation and stability models were updated with additional slosh dynamics, several simulations were performed to verify the impact of the mitigation strategies. In addition, stability analysis was repeated without the structural filter. Figures 17, 18 contain the Bode and Nichols plots of the systems with and without the structural filter. The removal of the structural filter increased the phase margin and reduced the modal suppression. However, the stability margins were not impacted in a detrimental manner. After the stability was validated and the mitigation strategies tested via simulation, the controller and operational changes were implemented in a composite burn, which is a combination of a long ACS burn to provide enough ΔV for the orbit raising and a short main engine burn to test the modified Delta-V mode. The AMF 5 composite burn consisted of a 40 minute, ACS thrusters only burn, and a 10 minute main engine burn. In addition, the anomaly investigation team found that the additional fill fraction data from the CFD analysis would improve the characterization of the slosh dynamics during the preflight analysis.

While the anomaly investigation team worked to find mitigation strategies, the maneuver team planned several ACS only maneuvers, the first of which was named AMF 2B.

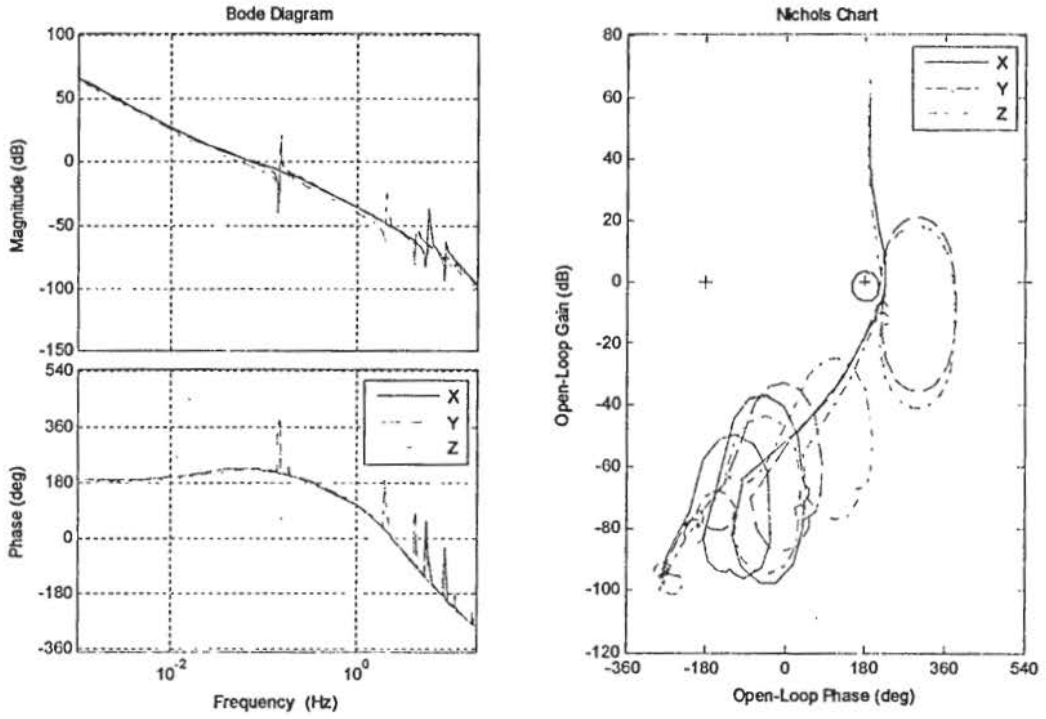

Figure 17. AMF 2A

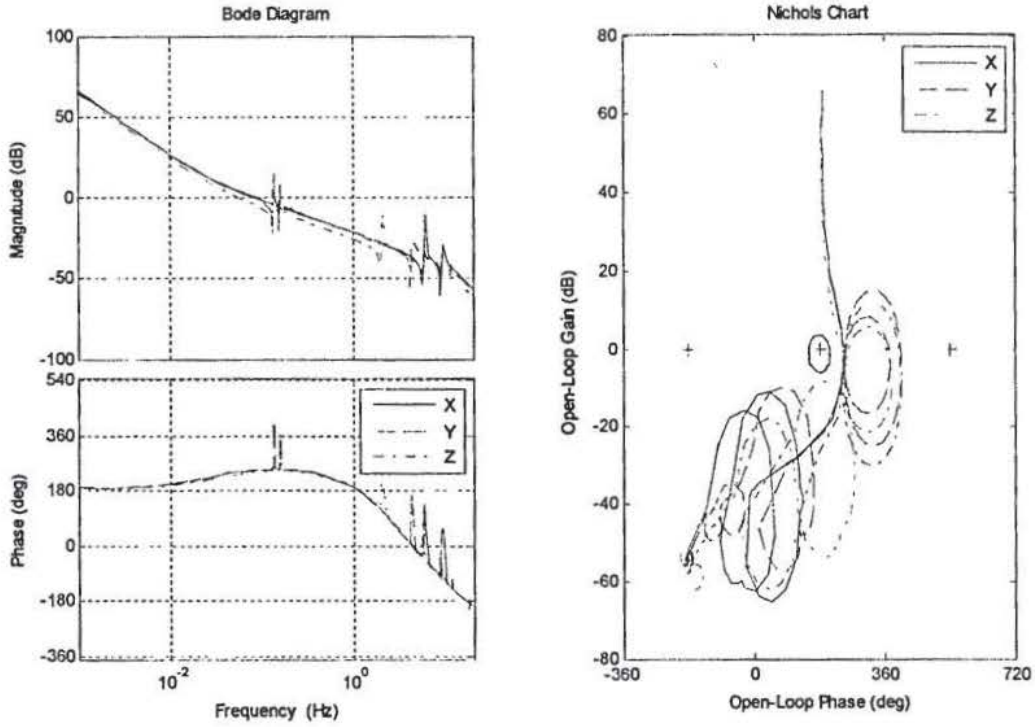

Figure 18. AMF 5 (Structural Filter Deactivated)

4. AMF 2B burn

AMF 2B was the first burn after the anomaly and consisted of a 20 minute ACS thruster only burn with ACS thrusters controlling in an off-pulsing manner. The total mass at the start of the burn was 2783.4 kg. The initial fill fraction was 75%.

The attitude errors for AMF 2B did not have the z-axis hang-off that is due to the main engine alignment and the CM offset (Figure 19). However, the y-axis hang-off is about the same. Based on analysis, the 5-lbf ACS thrusters' misalignments, which are bounded at 0.5 degrees, are not significant contributors to the hang-off. Therefore, it can be inferred that there is a CM offset in the z direction that produces the attitude hang-off in the y-axis. Because the attitude profile is noisy in the z axis, it is difficult to determine any significant CM offset in the z-axis. At 2800 seconds there is a pause in the oscillations, which was due to the thruster control resolution and the roll attitude hovering near zero. The system momentum initially peaks at 15 Nms, but settles to values below 11 Nms (Figure 20). The disturbance torque oscillations have an amplitude of approximately 7 Nm (3 sigma). The PSD of the disturbance plots resulted in a roll and yaw frequency of 0.1 Hz. The pitch frequency was 0.5Hz.

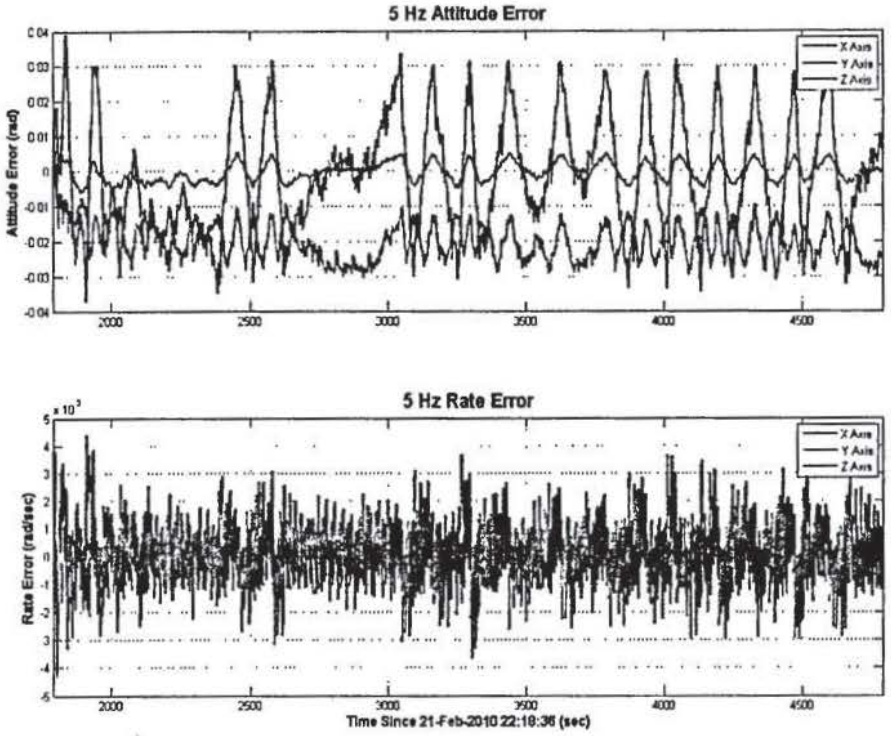

Figure 19. Attitude and Rate errors

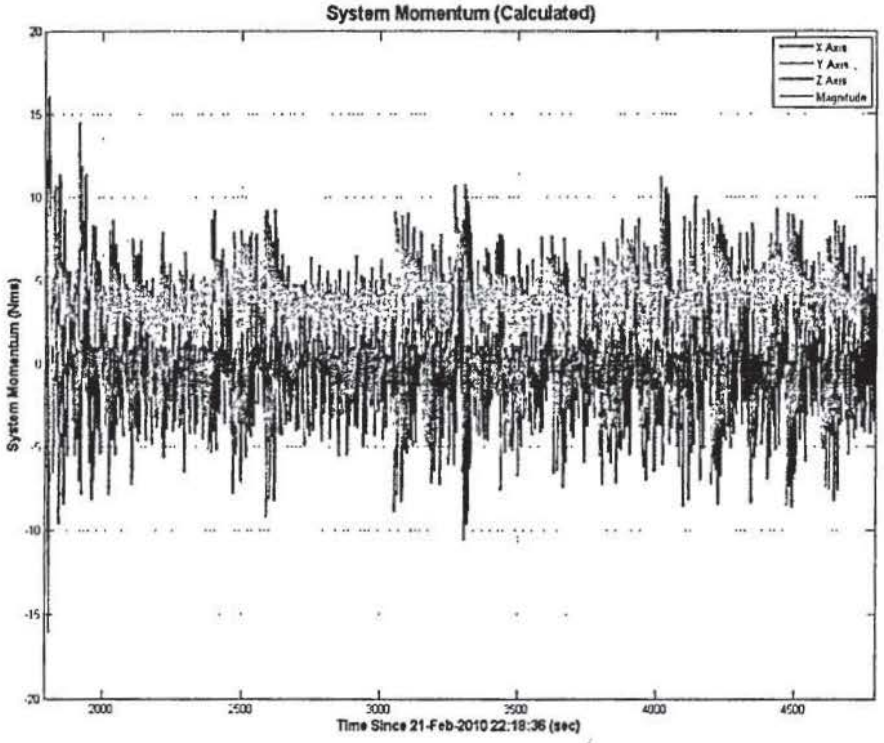

Figure 20. System momentum

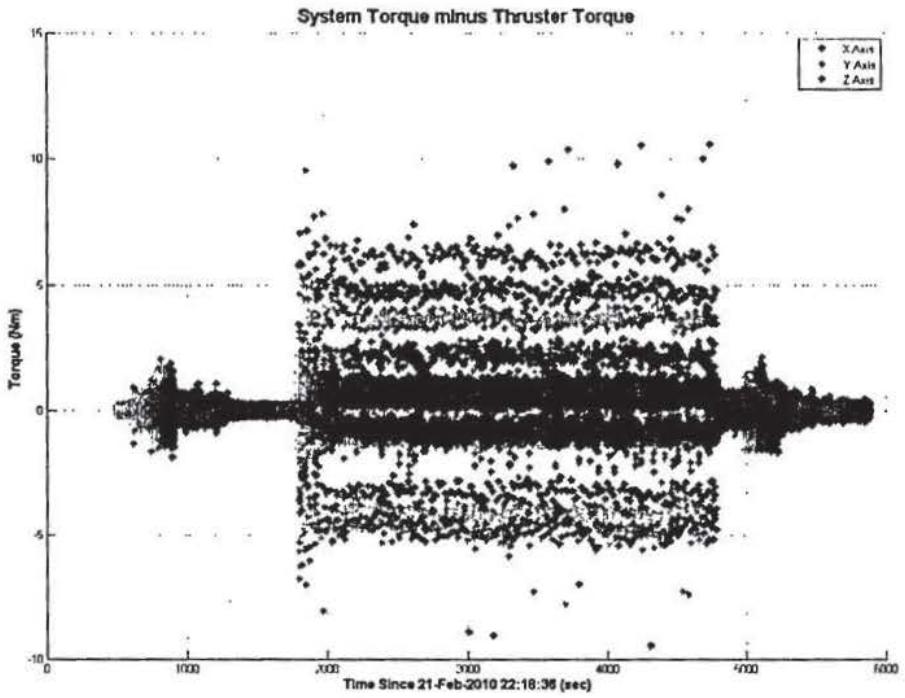

Figure 21. Disturbance torques

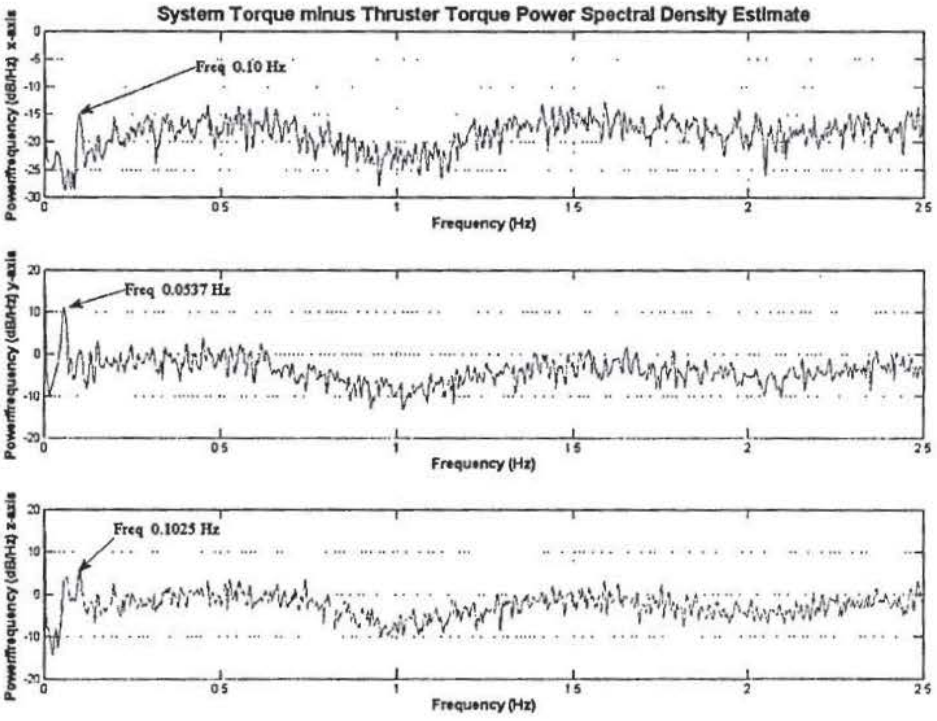

Figure 22. PSD of disturbance torques

5. AMF 5 composite burn

AMF 5 consisted of a 40 minute ΛCS thruster only burn followed by a 10 minute main engine burn with ACS thrusters controlling in an on-pulsing manner. This combination was called a composite burn in that the settling burn time was extended, and the main engine time was decreased, so that the settling burn provided an appreciable amount of the needed ΔV. The total mass at the start of the burn was 2506 kg. The initial momentum state was below 5 Nms and the fill fraction was 51%. The attitude errors for the extended settling burn contained a hang-off similar to that of AMF 1 main engine burn. Comparing both burns, it can be inferred that this attitude hang-off was due to the CM offset (Figure 23). At the transition to the main engine the oscillations in the attitude errors decreased while the hang-off increases slightly. In addition, the attitude error deviations are smaller. The rate errors before the main engine ignition are much noisier than those after the ignition. The system momentum has a similar trend (Figure 24). Due to the higher accelerations at the transition to the main engine, the frequency of the rates and system momentum increases and the magnitude decreases. The disturbance torque plot (Figure 25) has the same transition point for the dynamics. At the transition point, the disturbance torques decrease by at least a factor of two. The PSD of the disturbance torque identifies one mode that was close to the power amplitude threshold at about 0.15Hz (0.942 rad/sec).

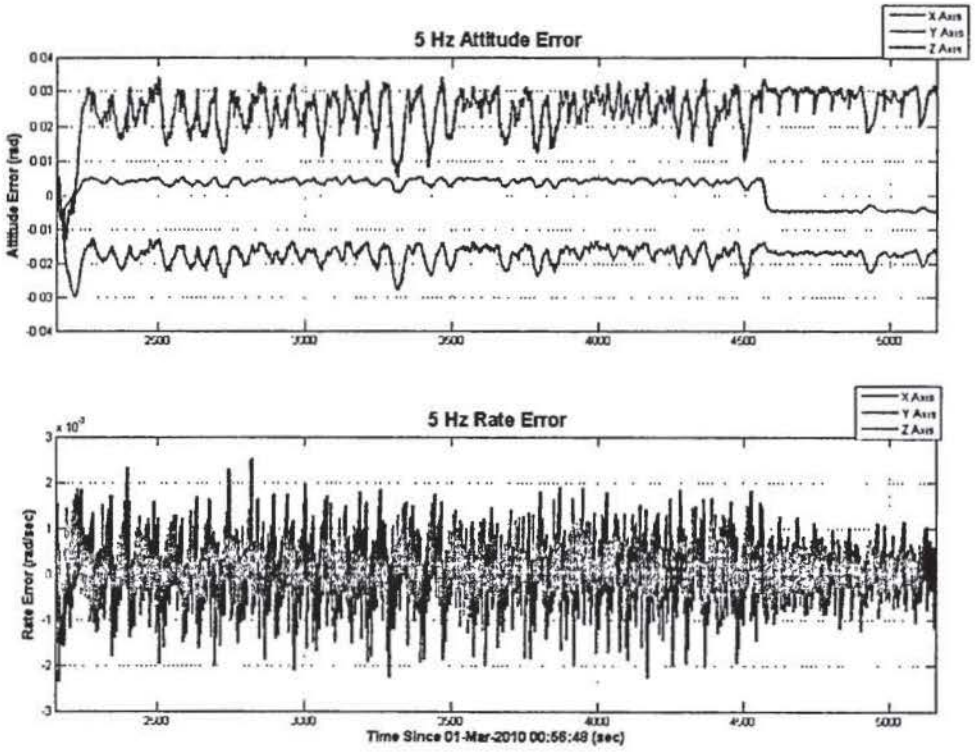

Figure 23. Attitude and Rate errors

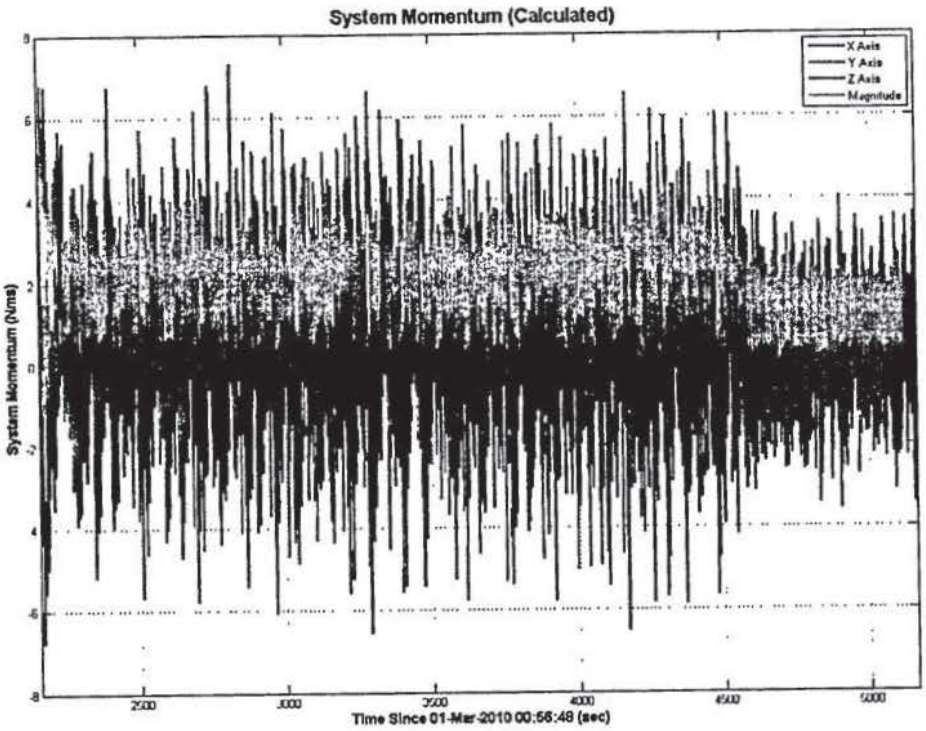

Figure 24. System momentum

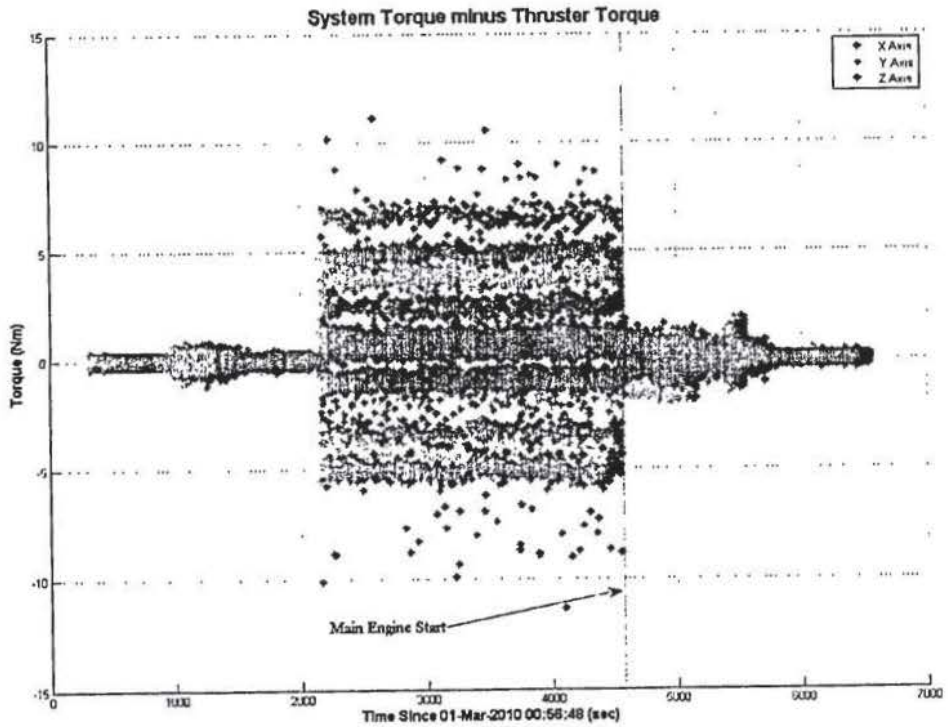

Figure 25. Disturbance torques

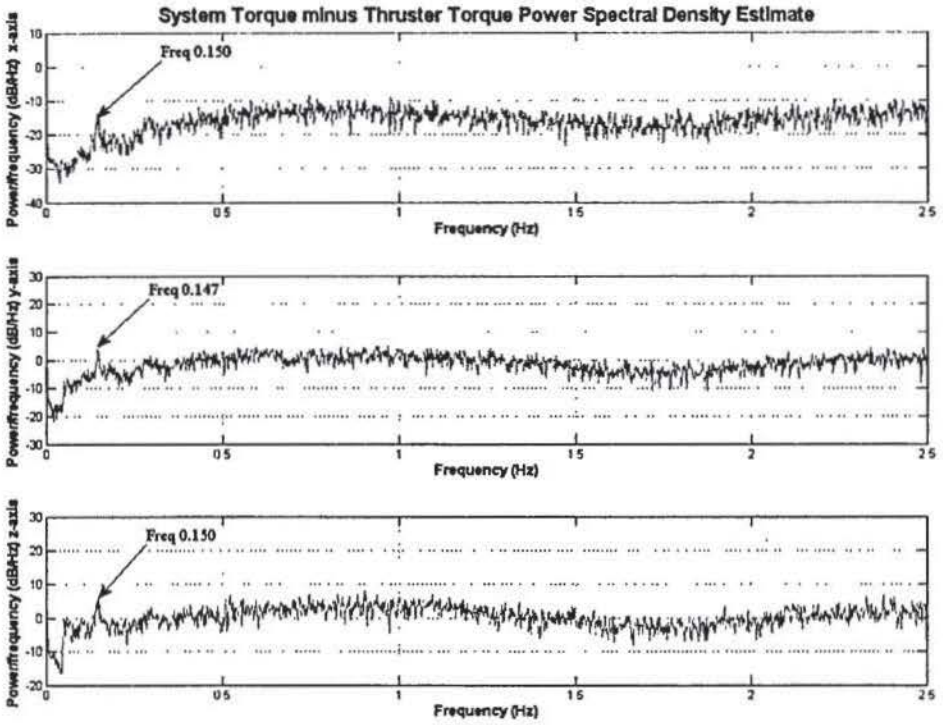

Figure 26. PSD of disturbance torques

6. AMF 6 burn

AMF 6 was the first maneuver where the slosh mitigation strategies were fully implemented. This burn consisted of a 4-minute ACS thruster-only burn followed by a 12.73 minute main engine burn. The total mass at the start of the burn was 2106 kg. The initial momentum state was below 5 Nms and the fill fraction was 43%.

The attitude errors for AMF 6 were similar to those of the previous maneuvers. However, the variations were smaller (Figure 27). This result is due to the removal of the structural filter. In addition, the roll hang-off switched sign. At the transition to the main engine the magnitude of oscillations in the attitude error hang-off remained the same. The system momentum was significantly smoother than the previous maneuver (Figure 28). After the transition between ACS and main engine, the disturbance torque dropped significantly (Figure 29). This was likely due to higher accelerations of a lighter spacecraft. The peak disturbance torque was 12 Nm before the transition and 3 Nm after.

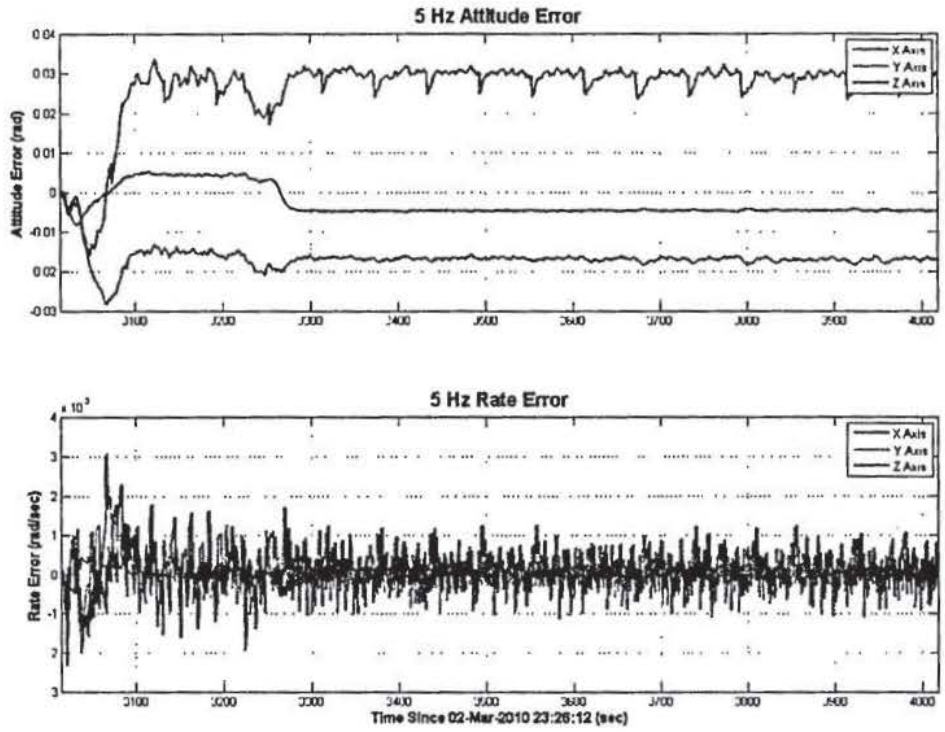

Figure 27. Attitude and Rate errors

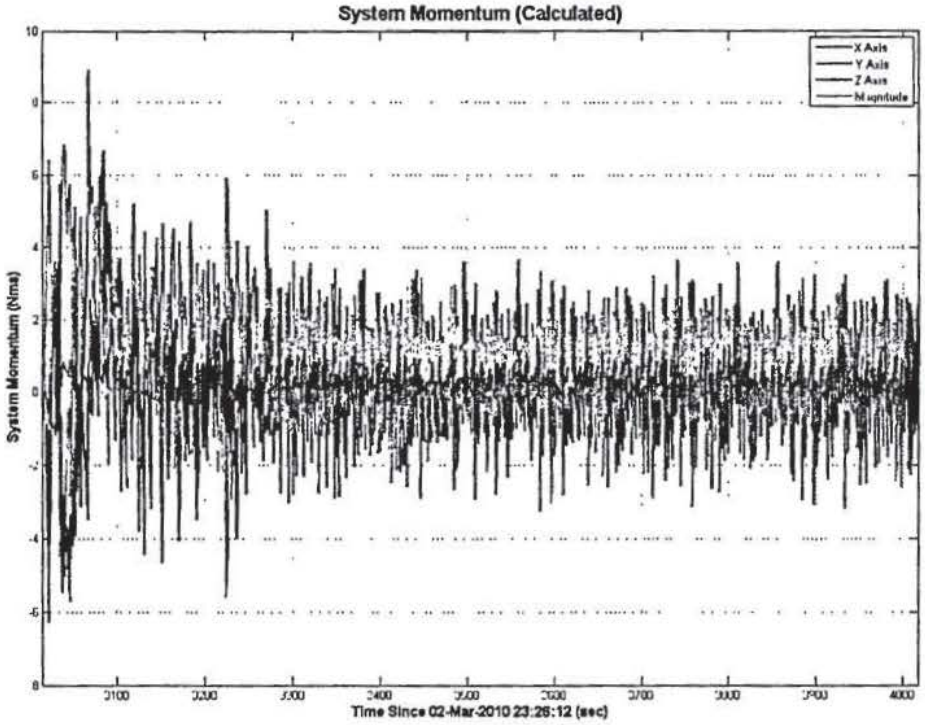

Figure 28. System momentum

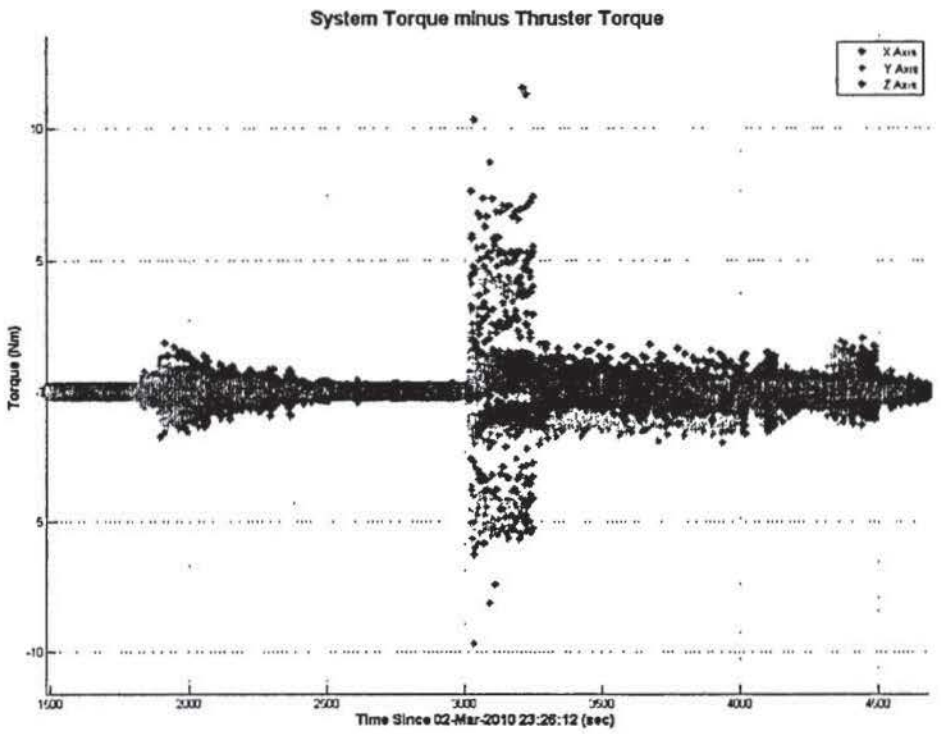

Figure 29. Disturbance torques

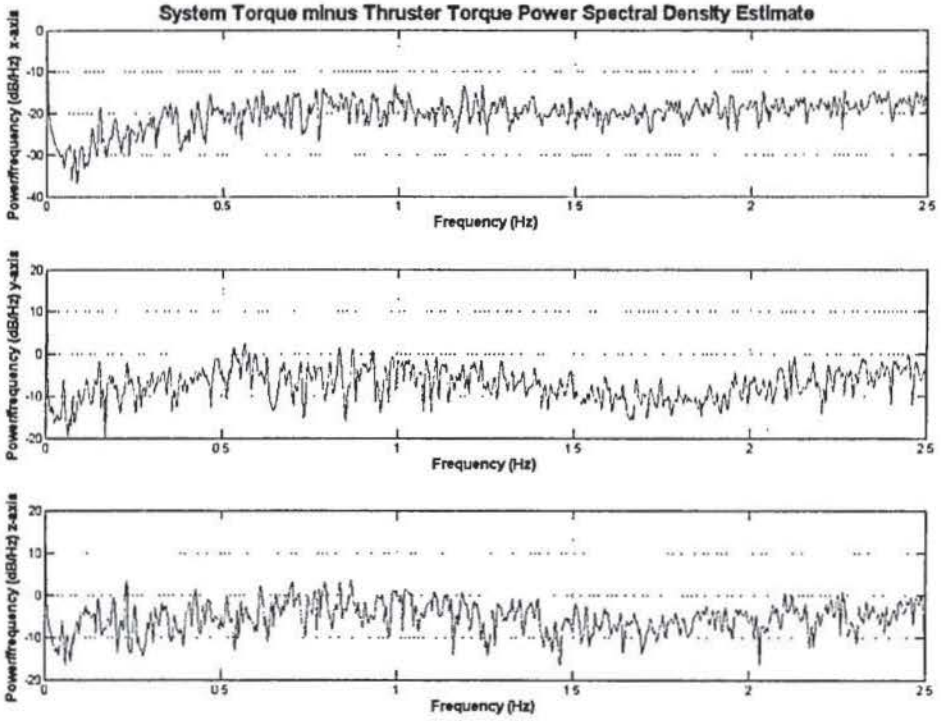

Figure 30. PSD of disturbance torques

C. Flight Results Conclusions

The first AMF maneuver performed as expected. Using the attitude hang-off (for various burn configurations) and the duty cycles, it is possible to distinguish between CM offset and misalignment. Because of the high fill fraction level in AMF 1, the initial dynamics were very comparable to the bare (empty) tank slosh dynamics. After the maneuver, both tanks were at an 81% fill fraction level. Thirty-seven seconds into the second AMF maneuver, the momentum levels exceeded 20 Nms and tripped a Fault Detection and Correction (FDC) limit, which aborted the burn and transitioned the spacecraft into Sun Acquisition mode. After the Sun Acquisition mode placed the spacecraft into a Sun-safe attitude, an anomaly investigation team was assembled to investigate the cause of the aborted burn. While the anomaly investigation was investigating the cause of the aborted burn, the rest of the SDO team designed a new GTO maneuver plan with ACS thrusters only. After the anomaly, three burns were performed using only the ACS thrusters (AMF 2B, AMF 3, and AMF 4). These burns all behaved in a similar manner.

After a lot of intense scrutiny, the cause of the anomaly was determined to be slosh. The anomaly investigation determined that a longer settling burn of four minutes was needed along with higher momentum limits and an update to the Delta-V structural filter parameters to make the filter a unity pass-through. The Delta-V mode structural filter, used for modal suppression, added a time delay into the system and diminished the controller's ability to compensate for the slosh. Once these solutions were validated in simulation, the appropriate changes were made in the flight software and the flight dynamics team designed a new maneuver plan that incorporated the main engine AMF 5. At the start of the AMF 5, the fill fraction was 51%. As the fill fraction dropped, the modal mass decreased. Below 40% fill fraction the PMD starts to impact the dynamics of the slosh. The mitigation strategies used in AMF 5 (and future maneuvers) performed better than expected. The FDC momentum limit never came close to tripping. The removal of the structural filter and increased settling time resulted in a smoother response, and the later main engine maneuvers (AMF 6, 7, and 8) performed better than AMF 1.

V. Post-Launch Lessons Learned

As a result of the SDO flight experience, the following lessons have been learned: First, the settling burn interval, which was defined by the geyser slosh mode, needs to also account for the dominant lateral slosh mode period. The dominant mode can vary as a function of fill fraction and tank geometry. For SDO the settling burn should be a function of the largest settling time over the fill fraction range of 95% to 45%. Below this fill fraction range the PMD dynamics strongly damps the slosh dynamics.

The second lesson learned was that the structural filter was designed to reduce the dynamic effects from the low-frequency (~1 Hz) flexible-body modes, but it also introduced additional time delay in the closed-loop system. Both time delay and propellant slosh can reduce the robustness of the control system as well as degrade the attitude performance. The flexible-body modes were modeled with a very conservative damping ratio of 0.1%. Future designs should consider larger damping ratios for low-frequency, appendage modes (based on past experience) and a structural filter design that introduces less time-lag in the system (or the exclusion of the structural filter).

The third lesson learned was that the equivalent mechanical models may not be sufficient to capture the coupled fluid-structural dynamics. Therefore, additional modeling techniques or fill fraction dynamical parameters are needed to fully characterize the slosh dynamics over all fill fractions. This additional work may be a challenge in terms of time and budget for an analysis team, but for missions with very large wet-to-dry mass ratios, it may pay off very efficiently in smooth on-orbit operations.

VI. Conclusion

The SDO preflight propellant tank slosh analysis was used to identify potential slosh issues and investigate possible solutions. For SDO, the resulting slosh dynamics were the driving factor in the redesign of the PMD. The proposed PMD was expected to greatly increase the damping and reduce the center of mass motion, improving stability and performance. Computational fluid dynamics (CFD) was used to update the linear equivalent slosh model. This model was incorporated into the simulations to verify the performance and stability of the controller design. In hindsight, the equivalent mechanical model only captures one of the important modes. In addition, the model parameters were not determined for the full range of fill fractions, which led to inaccuracies in the model at higher fill fractions.

Because of the high fill fraction level during the second perigee-raising maneuver (AMF 2A), the initial dynamics were very comparable to the bare tank (i.e. no PMD) slosh dynamics. As a result, an anomaly occurred in which propellant motion caused the system to perceive a high angular momentum condition that was, in fact, false. After the anomaly, three burns (AMF 2B, AMF 3, AMF 4) were performed on ACS thrusters only. These maneuvers produce less acceleration and therefore smaller slosh torques. As the fill fraction decreased during these

subsequent burns, additional complex dynamical behavior was observed. The data from the various maneuvers shows changes in the slosh period and damping as the propellant was depleted. After careful analysis, a decision was made to null the structural filter in the controller, to lengthen the setting burn, and to attempt under these conditions to use the main engine for AMF 5. At the start of AMF 5, the fill fraction was 51%. As the fill fraction drops, the modal mass decreases. Below 40% fill fraction the PMD more strongly impacted the dynamics of the slosh. After successfully reaching orbit, SDO has performed successfully for its first year and a half. In that time, reflection on lessons learned has led to this paper and to mitigation strategies that should be considered during the design phase of future missions. The next paper from this body of work will provide a detailed analysis to explain why the anomaly occurred.

Acknowledgments

The authors would like to thank the SDO ACS, Maneuver, GNC, Flight Software and Mission Operations teams. The SDO team poured their time and energy into this and many other challenges to ensure mission success.

References

[1] W. Morgenstern, K. Bourkland, O. C. Hsu, A. Liu, P. Mason, J. R. O'Donnell, A. M. Russo, S. R. Starin, M. F. Vess. Solar Dynamics Observatory Guidance, Navigation, and Control System Overview. AIAA Guidance, Navigation, and Control Conference, 8-11 August 2011, Portland, Oregon. (to be published)

[2] H. F, Bauer "Stability Boundaries of Liquid Propellant Space Vehicles with Sloshing", AIAA Journal 1963., Vol. 1 no.7.

[3] H. N, Abramson "Dynamic Behavior of Liquids in Moving Containers", NASA, 1966, NASA SP-106.

[4] R.J., Hung and H.L. Pan "Modeling of Sloshing Modulated Angular momentum Fluctuations Actuated by Gravity Gradient Associated with Spacecraft Slew Motion", Appl. Math, Modeling, 1996, Vol. 20 May, p. 399-409.

[5] R., Buseck and H., Benaroya, "Mechanical Models for Slosh of Liquid Fuel", AIAA -93-1093

[6] J. R. Roberts, E.R. Basurto, and P. Chen "Slosh Design Handbook I", Northrop Space Lab, NASA Technical Report No. 27, Contract NAS8-11111.

[7] K. W. London "A fully coupled Multi-Rigid-Body Fuel Slosh Dynamics model applied to the TRIANA Stack", 2001 Flight Mechanis Symposium, NASA GSFC

[8] K. J. Walchko "Robust Nonlinear Attitude Control with Disturbance Compensation", Thesis (Ph. D.) University of Florida, 2003.

[9] W Morgenstern "Control of the Triana Spacecraft in the Presence of Fuel Slosh Dynamics", December 1, 1999.

[10] F. T., Dodge "The New Dynamic Behavior of Liquids in Moving Containers", 2000, NASA SP-106 update.

[11] N. Ottenstein, G. Natanson, R. McIntosh, J. Hashmall, S. Shulman, R., DeFazio, S. Starin, K. Bourkland, P. Mason, and M. Vess. "Solar Dynamics Observatory (SDO) Ascent Planning and Momentum Management." Space Ops 2010, Huntsville, AL, 2010.